

A novel multi lines analysis tool of Ca^{2+} dynamics reveals the nonuniformity of Ca^{2+} propagation

Akitoshi Miyamoto^{a,b,*}, Katsuhiko Mikoshiba^{a,*}

^aLaboratory for Developmental Neurobiology, Center for Brain Science, RIKEN, 2-1 Hirosawa, Wako-shi, Saitama, Japan

^bLaboratory of Single-Molecule Cell Biology, Kyoto University Graduate School of Biostudies, Kyoto, Japan

ARTICLE INFO

Keywords:

Ca^{2+} propagation
Velocity of Ca^{2+} propagation
Direction of Ca^{2+} propagation
ImageJ-Plugin

ABSTRACT

Extracellular stimuli evoke a robust increase in the concentration of intracellular Ca^{2+} ($[\text{Ca}^{2+}]_c$) throughout the cell to trigger various cellular responses, such as gene expression and apoptosis. This robust expansion of $[\text{Ca}^{2+}]_c$ is called Ca^{2+} propagation. To date, it is thought that intracellular second messengers, such as inositol 1,4,5-trisphosphate (IP_3) and intracellular Ca^{2+} , and clusters of IP_3 receptors (IP_3Rs) regulate Ca^{2+} propagation. However, little is known about how the elevation in the $[\text{Ca}^{2+}]_c$ spreads throughout the cell, especially in non-polar cell, including HeLa cell. In this study, we developed a novel multi lines analysis tool. This tool revealed that the velocity of Ca^{2+} propagation was inconstant throughout cell and local concentration of intracellular Ca^{2+} did not contribute to the velocity of Ca^{2+} propagation. Our results suggest that intracellular Ca^{2+} propagation is not merely the result of diffusion of intracellular Ca^{2+} , and that, on the contrary, intracellular Ca^{2+} propagation seems to be regulated by more complicated processes.

1. Introduction

Ca^{2+} functions as a ubiquitous intracellular second messenger in many organisms [1,2]. The binding of extracellular ligands, such as neurotransmitters and hormones, to their receptors on the plasma membrane activates phospholipase C, following the production of the inositol 1,4,5-trisphosphate (IP_3). IP_3 allows the rapid release of Ca^{2+} from intracellular Ca^{2+} stores, endoplasmic reticulum (ER), through IP_3 receptors (IP_3Rs) [3,4]. This leads to a robust elevation in the concentration of intracellular Ca^{2+} ($[\text{Ca}^{2+}]_c$) that spreads throughout the cell. This expansion of $[\text{Ca}^{2+}]_c$ is called Ca^{2+} propagation. Ca^{2+} propagation is thought to be a key component to regulate various cellular functions, such as gene expression [5–7], neuronal activity [8], and apoptosis [9–11], according to extracellular stimuli [12]. Thus, deciphering “intracellular codes” contained in Ca^{2+} propagation is crucial to elucidate regulatory mechanisms of intracellular Ca^{2+} -driven cellular functions. Currently, intracellular second messengers, such as IP_3 and Ca^{2+} , and clusters of IP_3Rs are thought to regulate intracellular Ca^{2+} propagation [13,14]. However, there seems to be several variations in the regulation of Ca^{2+} propagation. For example, in polarized cell, such as pancreatic acinar cell, the state of Ca^{2+} propagation was not uniform [15]. This nonuniformity Ca^{2+} propagation in acinar cell was due to the heterogeneous distributions of mitochondria that buffered intracellular Ca^{2+} and Ca^{2+} release channel on the ER [16]. IP_3Rs

were concentrated in the apical region in acinar cell [15,17,18]. In addition, the unique localization of mitochondria that surrounded the pancreatic acinar granule region also contributed to the heterogeneous propagation of Ca^{2+} [19]. In contrast, little is known about the state of intracellular Ca^{2+} propagation in non-polar cell, such as HeLa cell, e.g., it is not well known whether the velocity of Ca^{2+} propagation is constant throughout the cell and local concentration of Ca^{2+} affects the velocity of intracellular Ca^{2+} propagation. To answer these questions, we developed a novel multi lines analysis tool that revealed the non-uniformity of the state of Ca^{2+} propagation. Our results suggest that there are more complicated regulatory mechanisms of Ca^{2+} propagation than those that are expected. Additionally, our tool would be a powerful tool for analyzing Ca^{2+} propagation in various cell types, including astrocytes in the central nervous system (CNS).

2. Materials and methods

2.1. Ca^{2+} imaging

To express a genetically encoded Ca^{2+} indicator: GCaMP6f [20] proteins in HeLa cells, pGP-CMV-GCaMP6f (Addgene #40755) plasmids were transfected with FugeneHD (Promega, USA). Twenty-four hours after transfection, the fluorescent intensity of GCaMP6f in HeLa cells was acquired using an IX83 inverted microscope (Olympus, Japan)

* Corresponding authors at: Laboratory for Developmental Neurobiology, Center for Brain Science, RIKEN, 2-1 Hirosawa, Wako-shi, Saitama, Japan.

E-mail addresses: miyamoto.akitoshi.2c@kyoto-u.ac.jp (A. Miyamoto), mikoshiba@brain.riken.jp (K. Mikoshiba).

<https://doi.org/10.1016/j.ceca.2019.01.001>

Received 23 October 2018; Received in revised form 15 December 2018; Accepted 3 January 2019

Available online 04 January 2019

0143-4160/© 2019 The Authors. Published by Elsevier Ltd. This is an open access article under the CC BY-NC-ND license

(<http://creativecommons.org/licenses/by-nc-nd/4.0/>).

equipped with UPlanFIN60Xoil, Nipkow disk confocal unit (CSU-X1) (Yokokawa, Japan), EM-CCD camera (iXon EM + DU-897) (Andor Technology, UK), 488 nm LD laser and the filter set for green fluorescent protein (Ex: FF02-472/30-25, DM: FF495-Di03-25 × 36, and Em: FF01-520/35-25, Semrock, USA). Ca^{2+} imaging was performed using a stream acquisition mode (exposure time was 30 ms and readout time of EM-CCD was about 30 ms) of MetaMorph (Molecular devices, USA). A balanced salt solution, containing 20 mM HEPES (pH 7.4), 115 mM NaCl, 5.4 mM KCl, 1 mM MgCl_2 , 10 mM glucose and 2 mM CaCl_2 was used for imaging, which was performed at room temperature (approximately 20 °C–23 °C). Offline analysis was performed using MetaMorph (Molecular device, USA), Fiji and Igor Pro software (WaveMetrics, USA).

2.2. Analysis of parameters during intracellular Ca^{2+} propagation

Our novel multi lines analysis tool is an ImageJ plugin written in Java (Oracle Corporation, USA). In this program, we can simultaneously draw several lines from the initiation site of Ca^{2+} propagation (Fig. 2A). Moreover, the initiation site of Ca^{2+} propagation can be manually determined. The angle between the lines can be modified in the range of 10°, 15°, 20°, 30°, and 45°. Thus, e.g., if the angle between the lines is set to 10° or 45°, 18 or 4 lines are drawn on the cell, respectively. In this study, we drew 12 lines (corresponding to 15°) to investigate the state of Ca^{2+} propagation. The IJ method (getPixelValue in Class FloatProcessor) was used to obtain the fluorescent intensity of GCaMP6f at each pixel on the line. To create graphical data (Fig. 2B), we used blank images as palettes (size = line length × number of slice images), where each pixel had a value of 0, and then the line analyzed data value was placed in each pixel using the IJ method (putPixelValue in Class ImagePlus). Additionally, our program exported the line analyzed data from each line into excel files for further analysis.

The velocity of Ca^{2+} propagation was calculated from the analyzed image using the following formula.

$$v = \text{pixel size} / \tan(\text{angle})$$

The pixel size was 267 nm, and the angle corresponded to the angle between two white lines in Fig. 3A. Offline analysis was performed using custom-made ImageJ plugins, Fiji and Igor Pro software.

Someone who wants to use our novel analysis tool described here should contact us (A.M: miyamoto.akitoshi.2c@kyoto-u.ac.jp or K.M: mikosiba@brain.riken.jp).

2.3. Statistical analysis

A Pearson's correlation test was used for the measurement of the strength of a relationship between two variables.

3. Results

3.1. Ca^{2+} propagation did not spread evenly throughout the cell

Histamine induces the production of IP_3 , following the rapid and robust increase in the $[\text{Ca}^{2+}]_c$ in HeLa cells. To precisely analyze the state of expansion of intracellular Ca^{2+} in HeLa cells, we performed high-frequency imaging (about 16.7 Hz) of intracellular Ca^{2+} triggered by exposure to histamine using GCaMP6f [20] (Fig. 1A, and Supplementary movie 1). Treatment with 1 μM of histamine evoked a small local change in the intensity of GCaMP6f, corresponding to the initiation site of Ca^{2+} elevation, (white arrowhead in Fig. 1A), and the increase in GCaMP6f intensity gradually spread throughout the cell. This expansion of intracellular Ca^{2+} is known as Ca^{2+} propagation. Interestingly, several initiation sites appeared during Ca^{2+} propagation and contributed to the spread of intracellular Ca^{2+} .

Fig. 1B shows enlarged and binarized images of Ca^{2+} propagation initiated in the left part of the cell (corresponding to the region in the

red dotted box in Fig. 1A). Interestingly, we found that movements of the front line of Ca^{2+} propagation (red solid line in Fig. 1B) were not constant, suggesting that the velocity in the direction of Ca^{2+} propagation was nonuniform. This nonuniformity of Ca^{2+} propagation was clearly based on the inconstancy in the increment of spread area (blue line in Fig. 1C); although spread area of intracellular Ca^{2+} seemed to constantly increase (red line in Fig. 1C). Additionally, the total amount of $[\text{Ca}^{2+}]_c$ seemed to constantly increase, but the increment in the amount of $[\text{Ca}^{2+}]_c$ was inconstant (Fig. 1D). Further, no correlation was found between the increments in Ca^{2+} spread area and total amount of intracellular Ca^{2+} . Conversely, the fluctuations in the increments in Ca^{2+} spread area and that of total amount of $[\text{Ca}^{2+}]_c$ were opposed to each other (Supplementary Fig. 1). These results suggest that Ca^{2+} propagation was not only regulated by diffusion of intracellular Ca^{2+} but also by more complicated mechanisms.

3.2. Development of a novel line analysis tool for Ca^{2+} propagation

We attempted to further analyze the relationship between the direction and velocity of Ca^{2+} propagation. Unfortunately, proper tools to investigate the direction of Ca^{2+} propagation were not found, although there were several line analysis tools. The conventional line analysis using ImageJ plugin "Plot Profile" is not appropriate to analyze Ca^{2+} dynamics, because this plugin only shows a graph of line profile data and the graphical data are not accessible for further analysis. Hence, we developed a novel multi lines analysis tool to analyze intracellular Ca^{2+} propagation. This novel analysis tool allowed us to easily investigate several parameters of Ca^{2+} propagation, such as the local changes in $[\text{Ca}^{2+}]_c$, direction of Ca^{2+} propagation, and graphical data representing time-series changes in the fluorescent intensities of GCaMP6f proteins, of each line within seconds (Fig. 3A and B). Using these graphical data, we can calculate the velocity of Ca^{2+} propagation because the angle of Ca^{2+} propagation represents the velocity of Ca^{2+} propagation in each direction (Fig. 3A).

3.3. The tool revealed differences in the velocity in each direction

To address the velocity of Ca^{2+} propagation in various directions from the initiation site, we performed multi-lines analysis of 12 directions (0°, 15°, 30°, 45°, 60°, 75°, 90°, 105°, 120°, 135°, 150°, and 165°) (Fig. 2B). However, we here focused on only five directions from the initiation site (0°, 15°, 30°, 150°, and 165°; Fig. 3A) and analyzed the velocity of Ca^{2+} spread in each of those directions because they had long lengths of Ca^{2+} propagation. In contrast, the line analysis data from 45°, 60°, 75°, 90°, 105°, 120°, and 135° directions were too short to analyze the velocity of Ca^{2+} propagation. As expected from the results shown in Fig. 1B, the velocity of Ca^{2+} propagation was different in each direction (Fig. 3A). In this HeLa cell, the velocity of Ca^{2+} spread at 150° was fast ($v = 5.65 \mu\text{m/s}$), whereas at 0°, it was relatively slow ($v = 1.80 \mu\text{m/s}$). Additionally, many "hot spots" were noticed that had relatively high concentrations of $[\text{Ca}^{2+}]_c$ (red arrowhead in Fig. 3B). We hypothesized that the local Ca^{2+} concentration affects the velocity of Ca^{2+} propagation. To test this hypothesis, we analyzed the velocity of Ca^{2+} spread from each of the "hot spots" as well as Ca^{2+} concentration in each. No correlation between the local Ca^{2+} concentration and local velocity of Ca^{2+} propagation ($r = 0.1615$; Fig. 3C) was found. These results indicated that the local Ca^{2+} concentration was not the sole regulator of the Ca^{2+} propagation.

4. Discussion

In this study, we focused on the state of intracellular Ca^{2+} propagation that has remained unexplored. Through the use of a novel multi lines analysis tool, we revealed the nonuniformity of the state of Ca^{2+} propagation. Understanding the precise way of Ca^{2+} propagation has remained unknown due to the lack of proper analysis tools. There are

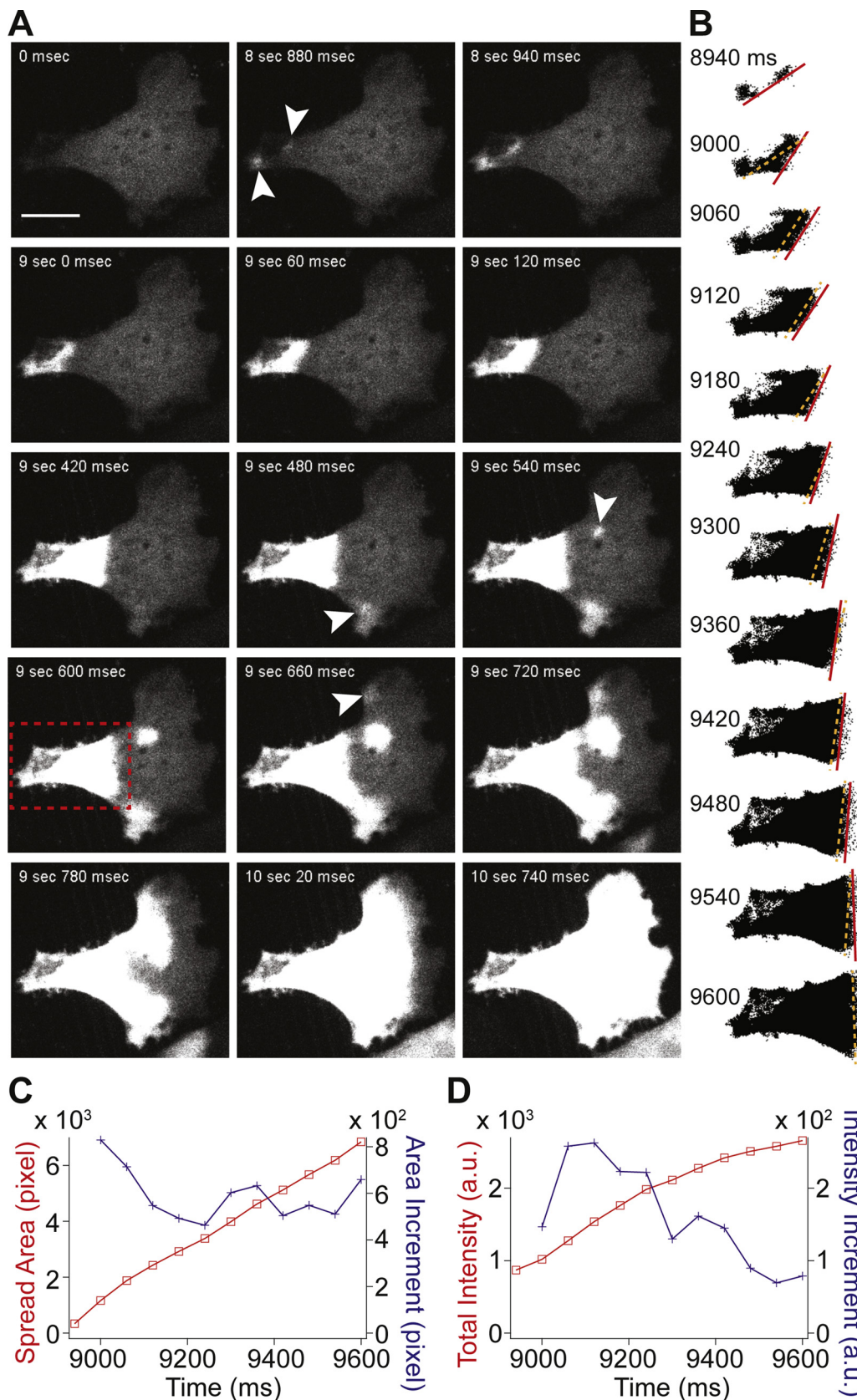


Fig. 1. Ca^{2+} propagation did not evenly spread throughout the cell. (A) GCaMP6f-expressing HeLa cells were stimulated with $1 \mu\text{M}$ of histamine (around 8 s). The white arrowhead indicates the initiation site of Ca^{2+} propagation in this and following figures. Scale bar represents $20 \mu\text{m}$. (B) Enlarged and binarized images of Ca^{2+} propagation initiated from the left part of the cell (red dotted box in Fig. 1A; from 8940 to 9600 ms of supplementary movie1). The red solid and orange dotted lines indicate the front line of Ca^{2+} propagation in the current and previous sections, respectively. (C) The temporal changes in the area of Ca^{2+} propagation. The red and blue lines indicate the area of Ca^{2+} propagation and area increment in each section, respectively. (D) The temporal changes in the concentration of $[\text{Ca}^{2+}]_c$. The red and blue lines indicate the total amounts of $[\text{Ca}^{2+}]_c$ and $[\text{Ca}^{2+}]_c$ increments in each section, respectively.

various types of analysis tools, such as ImageJ plugin “Line Profile” to perform line analysis. However, this tool can only analyze single lines. Thus, it is not suitable for investigating differences in the velocity in various directions of Ca^{2+} propagation. But, our novel multi lines

analysis tool enabled us to easily investigate the velocity of Ca^{2+} propagation in each direction from the initiation site.

Currently, the local elevation in the intracellular Ca^{2+} concentration, called Ca^{2+} puff, is thought to induce the additional release of

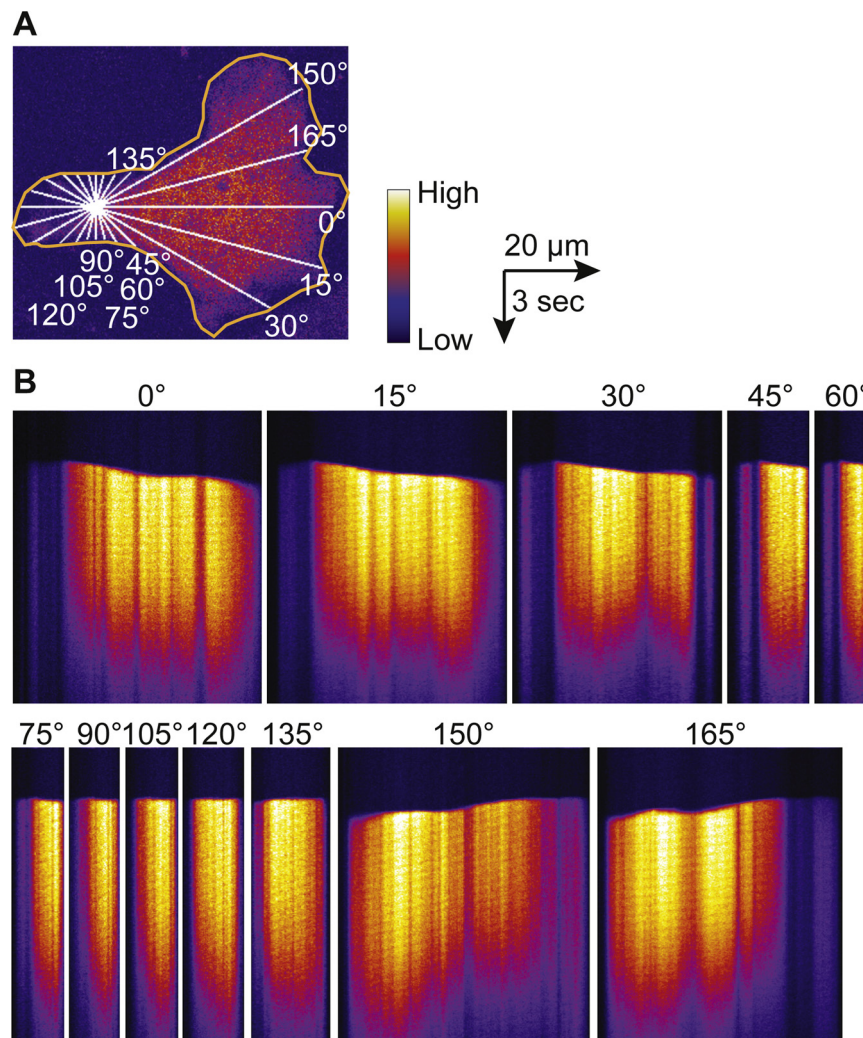


Fig. 2. The novel line analysis tool allowed us to observe differences of Ca^{2+} propagation in each direction. (A) An analyzed image showing the location of the line analysis. The white and orange lines indicate the analyzed line of each direction (from 0° to 165°) and cell shape, respectively. The point where all lines cross represents the initiation site of Ca^{2+} propagation. (B) The line analyzed results of each direction. The x and y axes represent the length (pixel size = 267 nm) and time (interval = 60 ms), respectively.

Ca^{2+} from the ER through neighboring IP_3Rs clusters [21]. Thus, the local concentration of Ca^{2+} seems to affect the spread of intracellular Ca^{2+} , especially the velocity of Ca^{2+} propagation. However, our results, showing that there is no correlation between the local Ca^{2+} concentration and velocity of Ca^{2+} spread, were opposite to this conventional hypothesis. In polarized cell, including pancreatic acinar cell, the distributions of Ca^{2+} release channel, such as IP_3R and ryanodine receptor, and Ca^{2+} buffering intracellular organelle (e.g., mitochondria) contributed to the nonuniformity of Ca^{2+} propagation [15,17,18]. However, the same nonuniform Ca^{2+} propagation also observed in non-polar cell, such as HeLa cell, in which Ca^{2+} release channels and mitochondria were uniformly distributed throughout the cell. Thus, Ca^{2+} propagation was not merely regulated by the concentration of second messengers, including intracellular Ca^{2+} , and clusters of IP_3Rs . We think that intracellular Ca^{2+} dynamics are regulated by the local environment surrounding the ER, such as organelle–organelle interactions (e.g., ER–mitochondria) and organelle–membrane structures interactions (e.g., ER–plasma membrane) and that regulation of the local environment is a key factor in the formation of intracellular Ca^{2+} signals (unpublished data; submitted). Investigating details of the novel regulatory mechanisms will be the main focus for a future study.

The novel multi-lines analysis tool would be a very powerful tool for investigating the functional roles of intracellular Ca^{2+} signals in

various cell types, especially astrocytes. Astrocytes are a type of glial cells in the CNS that communicate with hundreds of spines of neighboring neurons using fluctuations in the $[\text{Ca}^{2+}]_i$ in astrocytes [22–25]. This tool would help to elucidate the role of astrocytic Ca^{2+} signals in the regulation of neuronal activity. Thus, this novel tool would play significant role in this field of research.

5. Conclusion

Ca^{2+} propagation is not constant and is not simply controlled by the local concentration of intracellular Ca^{2+} . Our novel multi-lines analysis tool would be a very powerful tool to provide new insights regarding regulatory mechanisms involved in Ca^{2+} propagation.

Author contributions

A.M and K.M conceived and designed research. A.M performed research and analyzed the data. A.M and K.M wrote the manuscript.

Conflict of interest

The authors have no conflict of interest directly relevant to the content of this manuscript.

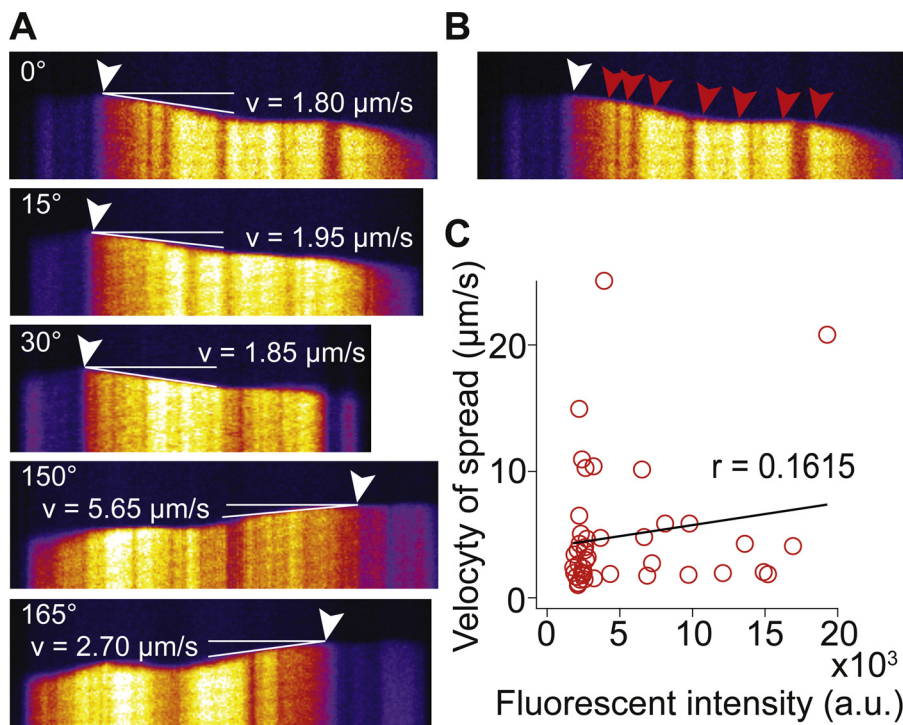


Fig. 3. The novel line analysis tool revealed differences in the velocity and direction of Ca^{2+} propagation. (A) The enlarged images of several line-analyzed data in Fig. 2B (0° , 15° , 30° , 150° and 165°). The white line indicates the angle of Ca^{2+} propagation that corresponds to the velocity of the Ca^{2+} spread (see Materials and Methods for details). (B) Representative image of “hot spots” in Ca^{2+} propagation. Red arrowheads indicate the hot spot. (C) The correlation between the local Ca^{2+} concentration and velocity of Ca^{2+} spread.

Acknowledgements

We are grateful to RIKEN BSI-Olympus Collaboration Center (BOCC) for imaging equipment and software. The authors would like to thank Enago (www.enago.jp) for the English language review. This work was supported by grants from the Ministry of Education, Culture, Sports, Science and Technology of Japan (20220007 to K.M) and RIKEN Incentive Research Project budget (100210 201701100431 to A.M).

Appendix A. Supplementary data

Supplementary material related to this article can be found, in the online version, at doi:<https://doi.org/10.1016/j.ceca.2019.01.001>.

References

- [1] M.J. Berridge, M.D. Bootman, H.L. Roderick, Calcium signalling: dynamics, homeostasis and remodelling, *Nat. Rev. Mol. Cell Biol.* 4 (2003) 517–529.
- [2] M.J. Berridge, Inositol trisphosphate and calcium signalling, *Nature* 361 (1993) 315–325.
- [3] H. Sugawara, M. Kurosaki, M. Takata, T. Kurosaki, Genetic evidence for involvement of type 1, type 2 and type 3 inositol 1,4,5-trisphosphate receptors in signal transduction through the B-cell antigen receptor, *EMBO J.* 16 (1997) 3078–3088.
- [4] J.K. Foskett, C. White, K.H. Cheung, D.O. Mak, Inositol trisphosphate receptor Ca^{2+} release channels, *Physiol. Rev.* 87 (2007) 593–658.
- [5] W. Li, J. Llopis, M. Whitney, G. Zlokarnik, R.Y. Tsien, Cell-permeant caged InsP_3 ester shows that Ca^{2+} spike frequency can optimize gene expression, *Nature* 392 (1998) 936–941.
- [6] R.E. Dolmetsch, K. Xu, R.S. Lewis, Calcium oscillations increase the efficiency and specificity of gene expression, *Nature* 392 (1998) 933–936.
- [7] T. Tomida, K. Hirose, A. Takizawa, F. Shibasaki, M. Iino, NFAT functions as a working memory of Ca^{2+} signals in decoding Ca^{2+} oscillation, *EMBO J.* 22 (2003) 3825–3832.
- [8] H. Bannai, F. Niwa, M.W. Sherwood, A.N. Shrivastava, M. Arizono, A. Miyamoto, K. Sugiura, S. Levi, A. Triller, K. Mikoshiba, Bidirectional control of synaptic GABAAR clustering by glutamate and calcium, *Cell Rep.* 13 (2015) 2768–2780.
- [9] A. Miyamoto, H. Miyauchi, T. Kogure, A. Miyawaki, T. Michikawa, K. Mikoshiba, Apoptosis induction-related cytosolic calcium responses revealed by the dual FRET imaging of calcium signals and caspase-3 activation in a single cell, *Biochem. Biophys. Res. Commun.* 460 (2015) 82–87.

- [10] S. Orrenius, B. Zhivotovsky, P. Nicotera, Regulation of cell death: the calcium-apoptosis link, *Nat. Rev. Mol. Cell Biol.* 4 (2003) 552–565.
- [11] M.W. Harr, C.W. Distelhorst, Apoptosis and autophagy: decoding calcium signals that mediate life or death, *Cold Spring Harb. Perspect. Biol.* 2 (2010) a005579.
- [12] M.J. Berridge, The AM and FM of calcium signalling, *Nature* 386 (1997) 759–760.
- [13] M.D. Bootman, P. Lipp, M.J. Berridge, The organisation and functions of local Ca^{2+} signals, *J. Cell. Sci.* 114 (2001) 2213–2222.
- [14] H. Qi, Y. Huang, S. Rudiger, J. Shuai, Frequency and relative prevalence of calcium blips and puffs in a model of small $\text{IP}(3)\text{R}$ clusters, *Biophys. J.* 106 (2014) 2353–2363.
- [15] H. Kasai, Y.X. Li, Y. Miyashita, Subcellular distribution of Ca^{2+} release channels underlying Ca^{2+} waves and oscillations in exocrine pancreas, *Cell* 74 (1993) 669–677.
- [16] M.C. Ashby, M. Craske, M.K. Park, O.V. Gerasimenko, R.D. Burgoyne, O.H. Petersen, A.V. Tepikin, Localized Ca^{2+} uncaging reveals polarized distribution of Ca^{2+} -sensitive Ca^{2+} release sites: mechanism of unidirectional Ca^{2+} waves, *J. Cell Biol.* 158 (2002) 283–292.
- [17] P. Thorn, A.M. Lawrie, P.M. Smith, D.V. Gallacher, O.H. Petersen, Local and global cytosolic Ca^{2+} oscillations in exocrine cells evoked by agonists and inositol trisphosphate, *Cell* 74 (1993) 661–668.
- [18] M.H. Nathanson, M.B. Fallon, P.J. Padfield, A.R. Maranto, Localization of the type 3 inositol 1,4,5-trisphosphate receptor in the Ca^{2+} wave trigger zone of pancreatic acinar cells, *J. Biol. Chem.* 269 (1994) 4693–4696.
- [19] H. Tinel, J.M. Cancela, H. Mogami, J.V. Gerasimenko, O.V. Gerasimenko, A.V. Tepikin, O.H. Petersen, Active mitochondria surrounding the pancreatic acinar granule region prevent spreading of inositol trisphosphate-evoked local cytosolic Ca^{2+} signals, *EMBO J.* 18 (1999) 4999–5008.
- [20] T.W. Chen, T.J. Wardill, Y. Sun, S.R. Pulver, S.L. Renninger, A. Baohan, E.R. Schreier, R.A. Kerr, M.B. Orger, V. Jayaraman, L.L. Looger, K. Svoboda, D.S. Kim, Ultrasensitive fluorescent proteins for imaging neuronal activity, *Nature* 499 (2013) 295–300.
- [21] M.Y. Sun, M. Geyer, Y.A. Komarova, IP_3 receptor signaling and endothelial barrier function, *Cell. Mol. Life Sci.* 74 (2017) 4189–4207.
- [22] G.R. Gordon, K.J. Iremonger, S. Kantevari, G.C. Ellis-Davies, B.A. MacVicar, J.S. Bains, Astrocyte-mediated distributed plasticity at hypothalamic glutamate synapses, *Neuron* 64 (2009) 391–403.
- [23] M.A. Di Castro, J. Chuquet, N. Liaudet, K. Bhaukaurally, M. Santello, D. Bouvier, P. Tiret, A. Volterra, Local Ca^{2+} detection and modulation of synaptic release by astrocytes, *Nat. Neurosci.* 14 (2011) 1276–1284.
- [24] N. Bazargani, D. Attwell, Astrocyte calcium signaling: the third wave, *Nat. Neurosci.* 19 (2016) 182–189.
- [25] N.J. Allen, C. Eroglu, Cell biology of astrocyte-synapse interactions, *Neuron* 96 (2017) 697–708.